JPET Fast Forward. Published on December 14, 2018 as DOI: 10.1124/jpet.118.253666
This article has not been copyedited and formatted. The final version may differ from this version.

Title:

Empagliflozin, an SGLT2 inhibitor, reduced the mortality rate after acute myocardial infarction with modification of cardiac metabolomes and anti-oxidants in diabetic rats.

Authors:

Hiroto Oshima*, Takayuki Miki*, Atsushi Kuno, Masashi Mizuno, Tatsuya Sato, Masaya Tanno, Toshiyuki Yano, Kei Nakata, Yukishige Kimura, Koki Abe, Wataru Ohwada, Tetsuji Miura

Affiliations:

Department of Cardiovascular, Renal and Metabolic Medicine (H.O., Ta.M., A.K., M.M., T.S., M.T., T.Y., K.N., Y.K., K.A., W.O., Te.M.), Department of Pharmacology (A.K.), and Department of Cellular Physiology and Signal Transduction (T.S.), Sapporo Medical University School of Medicine, Sapporo, Japan.

*These authors equally contributed to this study.

Running title: SGLT2 inhibitor and cardioprotection

Corresponding author:

Tetsuji Miura, MD, PhD

Department of Cardiovascular, Renal, and Metabolic Medicine

Sapporo Medical University School of Medicine

South-1, West-16, Chuo-ku

Sapporo 060-8543, Japan

Phone: +81-11-611-2111, ext. 32250

Fax: +81-11-644-7958

Email: miura@sapmed.ac.jp

Number of text pages: 18

Number of tables: 3

Number of figures: 7

Number of references: 42

Number of supplemental data: 2

Number of words in the abstract: 224

Number of words in the introduction: 651

Number of words in the discussion: 1496

List of nonstandard abbreviations:

BDH1, 3-hydroxybutyrate dehydrogenase 1; BNP, brain natriuretic peptide; CD36, cluster of differentiation 36; CPT1b, carnitine palmitoyltransferase 1b; DM, diabetes mellitus; FoxO3a, forkhead box O3a; F1,6P, fructose 1,6-diphosphate; F6P, fructose 6-phosphate; GLUT, glucose transporter; HDAC, histone deacetylases; HF, heart failure; LETO, Long-Evans Tokushima Otsuka rats; MCT1, monocarboxylate transporter 1; MI, myocardial infarction; OLETF, Otsuka Long-Evans Tokushima Fatty rats; PPAR, peroxisome proliferator-activated receptor; SCOT, succinyl-CoA:3-oxoacid CoA transferase; SGLT2, sodium glucose cotransporter 2; βOHB, β-hydroxybutyrate

A recommended section: Cardiovascular

Abstract

Background: Mechanism by which sodium glucose cotransporter 2 (SGLT2) inhibitors reduce cardiac events in diabetic patients remains unclear. Here we examined effects of an SGLT2 inhibitor on the acute survival rate after myocardial infarction (MI) in an animal model of type 2 diabetes mellitus (DM) and possible involvement of modification of cardiac metabolomes and anti-oxidative proteins.

Methods and Results: MI was induced in DM rats (OLETF) and control rats (LETO). Treatment with empagliflozin (10 mg/kg/day, 14 days) before MI reduced blood glucose and increased blood and myocardial β-hydroxybutyrate (βOHB) levels in OLETF. Survival rate at 48 hr after MI was significantly lower in OLETF than in LETO (40% vs 84%), and empagliflozin significantly improved the survival rate in OLETF to 70% though sizes of MI were comparable. Patterns of metabolomes and gene expression in the non-infarcted myocardium of OLETF were consistent with increased fatty acid oxidation and decreased glucose oxidation. The patterns were modified by empagliflozin, suggesting both increased glucose oxidation and ketone utilization in OLETF. Empagliflozin prevented reduction of ATP level in the non-infarcted myocardium after MI and significantly increased myocardial levels of Sirt3 and SOD2 in OLETF. Administration of βOHB partially mimicked the effects of empagliflozin in OLETF.

Conclusions: The results suggest that empagliflozin prevents DM-induced increase in post-MI mortality possibly by protective modification of cardiac energy metabolism and anti-oxidant proteins.

Introduction

Clinical studies have shown that heart failure (HF), in addition to atherosclerosis-related cardiovascular events, is a major cause of cardiovascular morbidity and mortality in patients with diabetes mellitus (DM) (Shah et al., 2015). DM increases the risk for the development of HF by more than two fold (Nichols et al., 2004), and patients with both HF and DM are at particularly high risk for adverse outcomes, regardless of coronary artery disease (Cubbon et al., 2013). Meta-analysis indicated that intensive glucose control does not prevent cardiac events and rather increased HF hospitalization compared with standard care (Udell et al., 2015). Recent clinical trials, however; have demonstrated that treatment with a sodium glucose cotransporter 2 (SGLT2) inhibitor significantly reduced cardiovascular events including HF hospitalization in patients with DM (Zinman et al., 2015; Neal et al., 2017).

How SGLT2 inhibitors prevent HF and death is not completely understood. Treatment of DM patients with SGLT2 inhibitors reduces plasma glucose level and also induces multiple hemodynamic, neurohumoral and metabolic changes that potentially influence cardiac pathology. Recently, the myocardial fuel hypothesis for cardioprotection afforded by SGLT2 inhibitors has received attention (Ferrannini et al., 2016b; Mudaliar et al., 2016), because SGLT2 inhibitors increase blood β-hydroxybutyrate (βOHB) levels (Min et al., 2018; Ferrannini et al., 2016a). Under physiological conditions, fatty acid and glucose are the main energy substrates in the heart, where energy sources are switched based on workload and substrate availability. However, HF is associated with decreased glucose oxidation and

increased fatty acid oxidation, leading to increased reactive oxygen species (ROS), in the myocardium (Lopaschuk et al., 2010; Lopaschuk. 2017). Since ketone bodies are more energy-efficient than free fatty acids, an increase in circulating ketone bodies is potentially beneficial for failing hearts. Indeed, ketone oxidation is increased in the failing heart (Aubert et al., 2016), and reduction of ketone utilization by cardiomyocyte-specific knockout of succinyl-CoA:3-oxoacid CoA transferase (SCOT), a key enzyme in ketone oxidation, resulted in adverse cardiac remodeling after pressure overload (Schugar et al., 2014). In addition, βOHB has been shown to suppress oxidative stress by inhibition of class I histone deacetylases (HDACs) (Shimazu et al., 2013). On the other hand, an association of increase in ketone bodies with adverse events has also been reported. In a study by Mizuno et al. (2017), cardiac uptake of ketone bodies was found to be increased in patient with DM, and the level of ketone uptake was positively correlated with plasma brain natriuretic peptide (BNP) level. Obokata et al. (2017) reported that increased serum βOHB level was associated with cardiovascular events and death in patients with renal failure. Thus, whether chronic elevation of circulating ketone bodies induced by an SGLT2 inhibitor is beneficial or detrimental in history of HF in DM patients remains uncertain.

In the present study, we examined the hypothesis that treatment with an SGLT2 inhibitor reduces mortality after MI by favorable effects on cardiac metabolomes and anti-oxidant proteins via increased plasma βOHB. To test the hypothesis, we used Otsuka Long-Evans Tokushima Fatty rats (OLETF) at ages of 25-30 weeks as a model of DM and we used empagliflozin as an SGLT2 inhibitor.

The reason for selection of OLETF in this study is three-fold. First, OLETF spontaneously develop DM primarily by hyperphagia due to a lack of cholecystokinin-A receptor in the brain and they show typical phenotype of type 2 DM (obesity, hyperinsulinemia and hypertriglyceridemia) (Bi et al., 2016; Murase et al., 2015). Second, ventricular dysfunction in OLETF was characterized in our previous studies (Takada et al., 2012; Kouzu et al., 2015), and shown to be similar to human diabetic cardiomyopathy. Third, we previously found that the mortality rate after MI in OLETF was significantly higher, due to lethal HF, than that in Long-Evans Tokushima Otsuka rats (LETO), non-DM control rats (Takada et al., 2012; Murase et al., 2015), and thus the beneficial effect of empagliflozin on DM-induced increase in post-MI mortality, if any, should be detectable.

Materials and Methods

The present study was conducted in strict accordance with the Guide for the Care and Use of Laboratory Animals published by National Research Council of the National Academies, USA (2011) and was approved by the Animal Use Committee of Sapporo Medical University.

Post-MI survival rate analysis: Protocol 1:

Experimental protocol is shown in Figure 1A. We used male OLETF and LETO rats, at ages of 25-30 weeks. Rats were pretreated with empagliflozin (10 mg/kg/day), an SGLT2 inhibitor, or a vehicle (dimethyl sulfoxide and polyethylene glycol; 1:1 vol:vol) for two weeks. Empagliflozin was kindly provided by Boehringer

Ingelheim (Ingelheim am Rhein, Germany). Empagliflozin and the vehicle were administered subcutaneously via osmotic minipumps (Alzet, Cupertino, CA, USA), not via drinking water containing the agents, because the amount of water that rats drink per day is not consistent. One day before induction of MI, systemic blood pressure and pulse rate were measured in a conscious state using a tail-cuff system (BP-98A, Softran, Tokyo, Japan) as in our previous study (Takada et al., 2012). After measurement of hemodynamics, each rat was lightly sedated with 3-4% isoflurane, and then the chest was shaved and the rat was placed in the supine position. Echocardiography was performed before induction of MI using a 11.5 MHz transducer connected to a Vivid-i Cardiovascular Ultrasound System (GE Medical, Milwaukee, USA) as previously reported (Takada et al., 2012; Murase et al., 2015, Kouzu et al. 2015).

After fasting for 12 hr, rats were anesthetized with isoflurane inhalation and then were intubated and ventilated with a rodent respirator (model 683, Harvard Apparatus, South Natick, MA). After small amount of blood was taken from tail vein for measurements of blood glucose and βOHB, the heart was exposed via left thoracotomy. Then a marginal branch of the left coronary artery was permanently ligated using a 5-0 silk thread to induce MI. Since empagliflozin could limit infarct size in ischemia-reperfusion model (Andreadou et al., 2017), we used a permanent occlusion model of MI to avoid inter-group differences in the infarct size and mechanical stress on the non-infarcted region of the hearts. The surgical wounds were repaired and the rats were returned to their cages. All rats were allowed ad-lib access to water but were restricted from food for 12 hr. Survival rates of rats in 4

groups (i.e., LETO, empagliflozin-treated LETO, OLETF, and empagliflozin-treated OLETF) were determined at 24 hr and 48 hr after MI. Rats that were alive at 48 hr after MI were euthanized by pentobarbital overdose, and heart tissue was excised. The excised heart was fixed in 10% formaldehyde and the size of infarction was analyzed by Azan staining and hematoxylin-eosin staining. Blood glucose and βOHB were measured using a Glutest-mint (Sanwa Kagaku Kenkyusho, Nagoya, Japan) and Presicion Xceed (Abbot, Chicago, IL), respectively.

Post-MI survival rate analysis: Protocol 2:

To examine the effects of exogenous βOHB on mortality, we subcutaneously administered βOHB (8.0 mmol/kg/day) or a vehicle to OLETF for 7 days before MI. After 12 hr of fasting, MI was induced as in protocol 1 (Figure 1B).

Tissue sampling protocol:

We previously reported that the mortality rate at 24-48 hr after MI was high (approximately 40%) in OLETF at ages of 25-30 weeks (Takada et al., 2012; Murase et al., 2015). Thus, myocardial tissue sampling for biochemical analyses was performed at 12 hr after MI (Figure 1). Since empagliflozin did not affect the survival rate of LETO (see Results), we used non-infarcted heart tissue samples from MI-induced rats (i.e., LETO, OLETF and empagliflozin-treated OLETF) to analyze changes associated with the empagliflozin-induced protection in this series of experiment. At 12 hr after MI, hearts were quickly excised and immediately soaked in ice-cold saline, and myocardium in the non-infarcted region was excised and

frozen in liquid nitrogen within 30 seconds. The samples were stored at -80˚C until use for biochemical analyses as in our previous studies (Takada et al., 2012; Murase et al., 2015). The hearts treated with a vehicle or βOHB in OLETF (protocol 2) were also sampled at 12 hr after MI.

Cellular signaling analysis

Frozen tissue samples were homogenized in ice-cold buffer (CelLyticTM MT Cell Lysis Reagent) including protease and phosphatase inhibitor cocktails (Nacalai Tesque, Inc., Kyoto, Japan). The homogenate was centrifuged at 15,000 g for 15 min at 4 ºC to obtain the supernatant. Equal amounts of protein were analyzed by immunoblot assays using specific antibodies (Supplemental Table 1). Intensities of individual bands were quantified by using Image J software (National Institutes of Health). mRNA quantification was performed as in our previous studies (Takada et al., 2012; Murase et al., 2015; Kouzu et al., 2015). Taqman gene expression assays and primer sequences were shown in Supplemental Table 1. ATP content in the non-infarcted myocardium was measured using an ATP colorimetric/fluorometric assay kit (BioVision). The formation of malondialdehyde (MDA) and 4-hydroxynonenal (4HNE), an indicator of lipid peroxidation, was examined using a Lipid Peroxidation Microplate Assay Kit (Oxford Biomedical Research, Oxford, MI).

Metabolome analyses

In this experiment, analysis was performed by Basic Scan and by C-Scope (Human Metabolome Technologies, Yamagata, Japan), according to the

recommended protocol (Makinoshima et al., 2014). Concentrations of extracted metabolites were measured by capillary electrophoresis time-of-flight mass spectrometry (CE-TOFMS) and capillary electrophoresis tandem mass spectrometry (CE-QqQMS; CE-MS/MS) as described previously (Makinoshima et al., 2014).

Statistical analyses

Data are presented as means ± SEM. Differences between treatment groups after MI were assessed by one-way analysis of variance (ANOVA). The Student-Newman-Keuls *post hoc* test was used for multiple comparisons when ANOVA indicated significant differences. Survival rates after MI were compared by Kaplan-Meier curves and log-rank statistics. For all tests, $p<0.05$ was considered statistically significant.

Results

Metabolic and hemodynamic profiles

Data for physiological profiles before induction of MI in the survival experiment are shown in Table 1. OLETF had larger body weight and higher fasting blood glucose than those of LETO, and treatment with empagliflozin reduced blood glucose level without affecting body weight in OLETF. Empagliflozin significantly increased βOHB level both in LETO and OLETF. Mean blood pressure, but not heart rate, in a conscious state was higher by 10~20 mmHg in OLETF than in LETO, and empagliflozin did not significantly change these parameters.

Echocardiography revealed that there were no differences in left ventricular

(LV) fractional shortening and LV wall thickness between LETO and OLETF, though LV dimension was larger in OLETF than in LETO before MI. Treatment with empagliflozin did not alter these echocardiographic parameters in either LETO or OLETF (Table 1). We tried to assess LV function after MI, but echocardiographic images of sufficient quality for analyses could not be obtained because of the surgical wound and remaining intra-thoracic air.

Data for metabolic and hemodynamic parameters before MI in the sampling experiment were similar to those in the survival experiment (data not shown). At 12 hr after MI (i.e., 24 hr of fasting), the levels of blood glucose and serum insulin were higher in OLETF than in LETO (Table 2). Treatment with empagliflozin significantly reduced blood glucose level but not serum insulin level in OLETF. The level of βOHB was slightly increased by continuation of fasting and by induction of MI in LETO and OLETF, and it was markedly increased in empagliflozin-treated OLETF. Levels of total cholesterol and triglyceride were higher in OLETF than in LETO and the change in the lipids was attenuated by empagliflozin. Acidosis was not induced by empagliflozin even after MI and 24 hr of fasting.

Infusion of exogenous βOHB did not change body weight and blood glucose, but significantly increased level of blood βOHB by approximately 30% in OLETF (Table 3). Exogenous βOHB slightly decreased blood pressure without affecting heart rate before MI in OLETF.

Survival rate after MI

The survival rate during a period of 48 hr after MI in LETO was 84.2%, and

pretreatment with empagliflozin for 2 weeks before MI did not affect the survival rate in LETO (88.2%) (Figure 2A). As in our previous studies (Takada et al., 2012; Murase et al., 2015), the survival rate was significantly lower in OLETF (40.0%) than in LETO. Pretreatment of OLETF with empagliflozin significantly increased the survival rate (70.4%, Figure 2A). Autopsies of rats that died within 48 hr after MI revealed lung congestion without cardiac rupture. Infarct sizes 48 hr after permanent coronary occlusion were 31%-37% of the left ventricle and were comparable among the treatment groups (Figure 2C).

In βOHB-treated OLETF, the survival rate was higher by 45% than that in vehicle-treated OLETF (76.2% vs. 52.6%, Figure 2B), though the difference did not reach statistical significance.

Myocardial levels of βOHB, ATP and BNP mRNA

βOHB levels in the non-infarcted myocardium after MI were similar in LETO and OLETF (190±33 and 184±31 nmol/g wet tissue, Supplemental Table 2). Treatment with empagliflozin significantly increased βOHB level in OLETF (1,719±670 nmol/g wet tissue). Myocardial ATP level after MI was significantly lower in OLETF than in LETO (3,550±502 vs 5,693±435 nmol/g wet tissue, Figure 2D). In contrast, ATP level was preserved in empagliflozin-treated OLETF after MI (5,719±789 nmol/g wet tissue). The preserved myocardial ATP level in empagliflozin-treated OLETF was similarly observed in metabolome analyses (see below and supplemental Table 2), though the difference did not reach statistical significance because of small number of samples in this analysis (n=4). In a

different set of experiment, we found that myocardial ATP level was not reduced after MI in βOHB-treated OLETF (5,216±1,023 nmol/g wet tissue, n=6). BNP mRNA level after MI in OLETF was slightly reduced by empagliflozin treatment, but there was not a statistical difference in BNP mRNA levels among 3 groups (Figure 2E).

Expression of genes that regulate glucose metabolism, β-oxidation and ketone oxidation

The mRNA levels of glucose transporter type 1 (GLUT1) and GLUT4 in the myocardium were not different between LETO and OLETF (Figure 3A, B). Empagliflozin did not affect these mRNA levels in OLETF. SGLT1 mRNA was detectable at similarly low levels in LETO and OLETF (data not shown) and SGLT2 mRNA was not detected in the myocardium. The mRNA levels of peroxisome proliferator-activated receptor (PPAR)-α and cluster of differentiation 36 (CD36) were higher in OLETF than in LETO, and empagliflozin treatment did not change these levels in OLETF (Figure 3C, D). On the other hand, the increased levels of both mRNA and protein of carnitine palmitoyltransferase 1b (CPT1b) in OLETF were attenuated by empagliflozin (Figure 3E, J). Expression of forkhead box O3a (FoxO3a) mRNA was increased in OLETF regardless of empagliflozin treatment (Figure 3F). Protein levels of 3-hydroxybutyrate dehydrogenase 1 (BDH1) and SCOT were not different among LETO, OLETF and empagliflozin-treated OLETF (Figure 3G, H). Monocarboxylate transporter (MCT) 1 protein, a transporter of lactate, pyruvate and ketone bodies, was also similarly expressed in the three groups (Figure 3I).

Metabolome analyses

Major metabolites relevant to energy metabolism in the non-infarcted region of the heart are shown in Figure 4. The levels of glucose 6-phosphate and fructose 1,6-diphosphate (F1,6P) were similar in OLETF and LETO. The ratio of F1,6P to fructose 6-phosphate (F6P) was significantly reduced in OLETF without MI (Kouzu et al., 2015), indicating suppressed phosphofructokinase, but such a change in the ratio of F1,6P to F6P was not observed in OLETF with MI in this series of experiments. On the other hand, lactate level and the lactate/pyruvate ratio were increased in OLETF, suggesting impaired glucose oxidation by reduced flux of pyruvate into the TCA cycle with diversion to lactate. Acetyl CoA levels were similar in LETO and OLETF, and the maintenance of acetyl CoA level in OLETF may be explained by increased β-oxidation, since the expression levels of PPAR-α, CD36 and CPT1b and protein level of CPT1b were increased in the myocardium (Figure 3C-E, J). Ketone bodies are unlikely to compensate for the diversion of pyruvate to lactate in OLETF since myocardial βOHB levels were similar in LETO and OLETF. Pentose phosphate pathway intermediates and ratios of NADPH to $NADP^+$ and reduced glutathione (GSH) to oxidized glutathione (GSSG) were not different in LETO and OLETF (Figure 4 and Supplemental Table 2). Levels of most TCA cycle intermediates (fumarate, malate, and citrate, but not succinate) were slightly decreased in OLETF. The decline in ATP in OLETF was associated with increased levels of ADP and AMP, and total adenylate levels were therefore comparable in LETO and OLETF.

In empagliflozin-treated OLETF, levels of 3-phosphoglyceric acid and phosphoenolpyruvic acid were similar to those in vehicle-treated OLETF, but pyruvate level was markedly reduced. The change in pyruvate level was accompanied by reductions in lactate level, lactate/pyruvate ratio and alanine level, suggesting that flux of pyruvate into the TCA cycle was increased by empagliflozin (Figure 4 and Supplemental Table 2). It is unlikely that β-oxidation of fatty acids contributed to the maintenance of acetyl CoA production in OLETF because mRNA and protein levels of CPT1b were reduced (Figure 3E, J) and lipid droplets in the cardiomyocytes were rather increased by empagliflozin (Mizuno et al., 2018). Therefore, increased myocardial βOHB level (Figure 4) might have contributed to acetyl CoA production, though lack of data for proteins and metabolites in the pathway from βOHB to acetyl CoA does not allow us to draw the conclusion regarding this point.

Anti-oxidant proteins and ROS production

The level of MDA+4HNE in the non-infarcted myocardium after MI was significantly higher in OLETF than in LETO, and this increase in OLETF was attenuated by treatment with empagliflozin (Figure 5A). Protein levels of superoxide dismutase 2 (SOD2) were similar in OLETF and LETO, but catalase level was lower in OLETF (Figure 5B, C). Empagliflozin treatment increased SOD2 level and partially restored catalase level in OLETF. The level of acetylated histone H3 was modestly increased by empagliflozin, though the difference did not reach statistical significance (Figure 5D). The protein level of Sirt3, a mitochondrial sirtuin, in

OLETF was similar to that in LETO but was significantly increased by treatment with empagliflozin (Figure 5E). The effects of empagliflozin on MDA+4HNE level, anti-oxidant proteins and Sirt3 were mimicked by exogenous administration of βOHB in OLETF (Figure 6A-D).

Discussion

In the present study, treatment with empagliflozin for 2 weeks significantly improved survival rate of OLETF after acute MI (Figure 2A). We previously demonstrated that increased mortality during the acute phase of MI in OLETF is due to progressive HF but not lethal arrhythmia (Takada et al., 2012). Congestion of the lung but not cardiac rupture after MI was detected by post-mortem examinations in rats died before 48 hr after MI. Furthermore, BNP expression at 12 hr after MI in OLETF was slightly suppressed by empagliflozin (Figure 2E). Therefore, suppression of HF is the most likely explanation for reduction in mortality after MI in OLETF by empagliflozin.

Unlike its effect in DM patients (Zinman et al., 2015; Neal et al., 2017), a beneficial effect of empagliflozin on post-MI mortality was observed without a significant change in body weight, blood pressure or heart rate in OLETF (Tables 1, 2). Thus, we could exclude hemodynamic changes from mechanisms of alterations in myocardial metabolism by empagliflozin. Changes in patterns of myocardial metabolites by empagliflozin in OLETF are consistent with a notion that empagliflozin restored glucose oxidation, increased ketone oxidation and decreased fatty acid oxidation, leading to maintenance of ATP level in the myocardium of OLETF (Figures

2D, 4). In contrast, Verma et al. (2018) recently reported that empagliflozin increased the rate of glucose and fatty acid oxidation without change in the ketone oxidation rate in db/db mice. We do not have a clear explanation for the difference in empagliflozin-induced changes in cardiac metabolism between OLETF and db/db mice, but presence of MI-induced HF in this study might be involved. Nevertheless, both a study by Verma et al. (2018) and the present study indicate that empagliflozin affords beneficial effect on myocardial ATP level. In addition to the changes in energy substrate metabolism, suppression of oxidative stress was another important change in empagliflozin-treated OLETF, since major roles of oxidative stress in development of HF have been shown in animal models of HF and patients with HF (Münzel et al., 2015; Ayoub et al., 2017). We found that empagliflozin increased expression of anti-oxidant stress proteins and suppressed biomarkers of oxidant stress in the myocardium after MI in OLETF (Figure 5A-C). Exogenous infusion of βOHB partially mimicked the protective effects of empagliflozin on mortality, ATP level and oxidative stress after MI in OLETF (Figures 2B, 6). The findings support the notion that improved function of the non-infarcted myocardium after MI by suppression of myocardial oxidant stress underlay improvement of post-MI survival rate in empagliflozin-treated OLETF.

It has been shown that a failing heart switches main energy sources from fatty acid to glucose metabolism, which is more efficient fuel (Lopaschuk et al., 2010; Lopaschuk., 2017). However, when HF reduces glucose oxidation by reduction of pyruvate dehydrogenase activity, it leads to a mismatch between glycolysis and glucose oxidation (Diakos et al., 2016). On the other hand, ketone oxidation

increases to compensate for the decrease in acetyl CoA production in the failing heart (Aubert et al., 2016; Bedi et al., 2016). Recently, it has been reported that cardiac-specific overexpression of BDH1 was protective in mice, while knockout of SCOT was detrimental to HF induced by pressure overload (Schugar et al., 2014; Uchihashi et al., 2017). These results support the notion that promotion of ketone oxidation improves the energy metabolism in failing hearts. In the present study, myocardial βOHB level was not different in LETO and OLETF and there was no change in the protein level of MCT1, BDH1 or SCOT after MI in OLETF (Figures 3G-I, 4). Thus, the present model of MI-induced HF did not have up-regulated ketone oxidation in the myocardium in contrast to HF models in earlier studies (Aubert et al., 2016; Schugar et al., 2014; Uchihashi et al., 2017; Diakos et al., 2016; Bedi et al., 2016), possibly because the duration of cardiac overload (12 hr vs. 4-8 weeks), severity of HF (post MI vs. aortic banding model) and/or presence of DM were different. Nevertheless, treatment with empagliflozin increased blood and myocardial βOHB levels by approximately 2-fold and 10-fold, respectively, and the increased tissue level of βOHB was accompanied by preservation of ATP level after MI. These findings suggested the possibility that increased delivery of ketone bodies to the heart with ventricular dysfunction is beneficial in terms of energy metabolism even if the expression of MCT1, BDH1 and SCOT is not up-regulated. However, metabolic adaptation of the heart may change during much longer treatment with empagliflozin, since it has been reported that a chronic ketogenic state in mice decreased myocardial SCOT expression and prevented inhibition of fatty acid oxidation (Wentz et al., 2010).

Oxidative stress plays a major role in myocardial dysfunction in HF and complications of DM (Münzel et al., 2015; Niemann et al., 2017; Ayoub et al., 2017), and suppression of ROS improved LV function after MI (Kinugawa et al., 2000). Recent studies have shown that expression of antioxidant enzymes, including SOD2 and catalase, are increased by class I HDAC inhibitory action of βOHB via up-regulation of FoxO3a (Shimazu et al., 2013; Nagao et al., 2016). In the present study, myocardial SOD2 level was unchanged, but catalase level was lower in OLETF than in LETO (Figure 5B, C). Empagliflozin increased SOD2 level and restored catalase level in OELTF, though it had no significant effect on FoxO3a mRNA or acetylated histone 3 protein levels. On the other hand, Sirt3 protein level was significantly increased in empagliflozin-treated OLETF, and one of the functions of Sirt3 is up-regulation of SOD2 and catalase by deacetylation of FoxO3a (Tseng et al., 2014). Interestingly, administration of exogenous ketones mimicked up-regulation of Sirt3 and anti-oxidant protein expression, being consistent with a report that infusion of ketones increased Sirt3 protein expression in brain tissues (Yin et al., 2015). How infusion of βOHB up-regulated Sirt3 expression in OLETF is unclear. However, activation of nuclear respiratory factor 2 (Nrf2) has been reported to mediate upregulation of Sirt3 expression by ketones in non-cardiac cells (Satterstrom et al., 2015; Buler et al., 2016; Izuta et al., 2018). Mechanisms by which βOHB activates Nrf2 and other regulatory factors of Sirt3 expression in the myocardium remain to be further investigated.

Although activators of PPARs have been shown not only to normalize blood glucose level but also to ameliorate decreased glucose oxidation and increased fatty

acid oxidation in diabetic hearts, the agents failed to improve cardiac performance (Aasum et al. 2002, 2005; Carley et al. 2004). Treatment with insulin in isolated perfused hearts of db/db mice rather reduced ATP production by reduction of palmitate oxidation (Verma et al. 2018). As effects being distinct from the effects of PPAR activators and insulin, empagliflozin increased ketone utilization in OLETF, in addition to restoring glucose oxidation and decreasing fatty acid oxidation, and up-regulated anti-oxidant proteins (Figures 4, 5). Taken together, increased utilization of ketones and suppression of myocardial oxidant stress may play larger roles than improved glucose and fatty acid metabolism in empagliflozin-induced protection of diabetic hearts from acute mortality after MI.

There are limitations in the present study. First, although metabolome analysis provided abundant data for metabolites, this method does not allow direct measurement of the flux in metabolic pathways. Thus, the assessment of cardiac energy metabolism made in this study is interpretive. Isotope-labeling of metabolites in an isolated perfused heart preparation is a more rigorous method to determine metabolic fluxes, but it is difficult for an ex-vivo perfusion study to mimic the effects of SGLT2 inhibitors *in situ* condition because of lack of organ interactions, including ketone body supply from the liver and kidney to the heart. Second, a role of βOHB in empagliflozin-induced cardioprotection has not been clarified. Infusion of exogenous βOHB into OLETF mimicked the effect of empagliflozin on Sirt3 and anti-oxidant proteins, but its effect on myocardial metabolomes was not analyzed. Since it was technically difficult to elevate blood βOHB level by its infusion to the level of βOHB in empagliflozin-treated OLETF, we did not attempt to rigorously

compare the effects of exogenous βOHB and empagliflozin on myocardial metabolomes. Third, whether the cardioprotective effect of empagliflozin is dose-dependent and/or is glycemic control-dependent remained unclear. However, infusion of βOHB partly mimicked the effects of empagliflozin on anti-oxidant protein expression and on mortality after MI, without significant reduction in blood glucose, in OLETF. The findings are consistent with results of clinical trials arguing against the presence of a close relationship between level of glycemic control and effects of SGLT2 inhibitors on cardiovascular events (Zinman et al., 2015; Neal et al., 2017).

In conclusion, treatment with empagliflozin significantly attenuated DM-induced increase in acute mortality after MI in a model of type 2 DM. The protective effects of an SGLT2 inhibitor was independent of hemodynamic changes and hematopoiesis but associated with improved energy metabolism and up-regulation of anti-oxidative proteins in the remote region of post-MI hearts (Figure 7). How the changes in cardiac metabolism and anti-oxidant defense play roles in the protection afforded by empagliflozin against detrimental effect of DM on post-MI mortality warrants further investigation.

Authorship Contributions

Participated in research design: Miki, Miura.

Conducted experiments: Oshima, Miki, Kuno, Mizuno, Sato, Nakata, Kimura, Abe, Ohwada.

Performed data analysis: Oshima, Miki, Kuno, Sato, Tanno, Yano.

Wrote or contributed to the writing of the manuscript: Oshima, Miki, Kuno, Tanno, Miura.

References

Aasum E, Belke DD, Severson DL, Riemersma RA, Cooper M, Andreassen M, Larsen TS (2002) Cardiac function and metabolism in Type 2 diabetic mice after treatment with BM 17.0744, a novel PPAR-alpha activator. Am J Physiol Heart Circ Physiol 283:H949-957.

Aasum E, Cooper M, Severson DL, Larsen TS (2005) Effect of BM 17.0744, a PPARalpha ligand, on the metabolism of perfused hearts from control and diabetic mice. Can J Physiol Pharmacol 83:183-190.

Andreadou I, Efentakis P, Balafas E, Togliatto G, Davos CH, Varela A, Dimitriou CA, Nikolaou PE, Maratou E, Lambadiari V, Ikonomidis I, Kostomitsopoulos N, Brizzi MF, Dimitriadis G, Iliodromitis EK (2017) Empagliflozin limits myocardial infarction in vivo and cell death in vitro: role of STAT3, mitochondria, and redox aspects. Front Physiol 8:1077.

Aubert G, Martin OJ, Horton JL, Lai L, Vega RB, Leone TC, Koves T, Gardell SJ, Krüger M, Hoppel CL, Lewandowski ED, Crawford PA, Muoio DM, Kelly DP (2016) The failing heart relies on ketone bodies as a fuel. Circulation 133:698-705.

Ayoub KF, Pothineni NVK, Rutland J, Ding Z, Mehta JL (2017) Immunity, Inflammation, and Oxidative Stress in Heart Failure: Emerging Molecular Targets. Cardiovasc Drugs Ther 31:593-608.

Bedi KC Jr, Snyder NW, Brandimarto J, Aziz M, Mesaros C, Worth AJ, Wang LL, Javaheri A, Blair IA, Margulies KB, Rame JE (2016) Evidence for intramyocardial disruption of lipid metabolism and increased myocardial ketone utilization in advanced human heart failure. Circulation 133:706-716.

Bi S, Moran TH (2016) Obesity in the Otsuka Long Evans Tokushima Fatty rat: mechanisms and discoveries. Front Nutr 3:21.

Buler M, Andersson U, Hakkola J (2016) Who watches the watchmen? Regulation of the expression and activity of sirtuins. FASEB J 30:3942-3960.

Carley AN, Semeniuk LM, Shimoni Y, Aasum E, Larsen TS, Berger JP, Severson DL (2004) Treatment of type 2 diabetic db/db mice with a novel PPARgamma agonist improves cardiac metabolism but not contractile function. Am J Physiol Endocrinol Metab 286:E449-455.

Cubbon RM, Adams B, Rajwani A, Mercer BN, Patel PA, Gherardi G, Gale CP, Batin PD, Ajjan R, Kearney L, Wheatcroft SB, Sapsford RJ, Witte KK, Kearney MT (2013) Diabetes mellitus is associated with adverse prognosis in chronic heart failure of ischaemic and non-ischaemic aetiology. Diab Vasc Dis Res 10:330-336.

Diakos NA, Navankasattusas S, Abel ED, Rutter J, McCreath L, Ferrin P, McKellar SH, Miller DV, Park SY, Richardson RS, Deberardinis R, Cox JE, Kfoury AG, Selzman CH, Stehlik J, Fang JC, Li DY, Drakos SG (2016) Evidence of glycolysis up-regulation and pyruvate mitochondrial oxidation mismatch during mechanical unloading of the failing human heart: implications for cardiac reloading and conditioning. JACC Basic Transl Sci 1:432-444.

Ferrannini E, Baldi S, Frascerra S, Astiarraga B, Heise T, Bizzotto R, Mari A, Pieber TR, Muscelli E (2016a) Shift to fatty substrate utilization in response to sodium-glucose cotransporter 2 inhibition in subjects without diabetes and patients with type 2 diabetes. Diabetes 65:1190-1195.

Ferrannini E, Mark M, Mayoux E (2016b) CV Protection in the EMPA-REG OUTCOME trial: a "thrifty substrate" hypothesis. Diabetes Care 39:1108-1114.

Izuta Y, Imada T, Hisamura R, Oonishi E, Nakamura S, Inagaki E, Ito M, Soga T, Tsubota K (2018) Ketone body 3-hydroxybutyrate mimics calorie restriction via the Nrf2 activator, fumarate, in the retina. Aging Cell 17.

Kinugawa S, Tsutsui H, Hayashidani S, Ide T, Suematsu N, Satoh S, Utsumi H, Takeshita A (2000) Treatment with dimethylthiourea prevents left ventricular remodeling and failure after experimental myocardial infarction in mice: role of oxidative stress. Circ Res 87:392-398.

Kouzu H, Miki T, Tanno M, Kuno A, Yano T, Itoh T, Sato T, Sunaga D, Murase H, Tobisawa T, Ogasawara M, Ishikawa S, Miura T (2015) Excessive degradation of adenine nucleotides by up-regulated AMP deaminase underlies afterload-induced diastolic dysfunction in the type 2 diabetic heart. J Mol Cell Cardiol 80:136-145.

Lopaschuk GD (2017) Metabolic modulators in heart disease: past, present, and future. Can J Cardiol 33:838-849.

Lopaschuk GD, Ussher JR, Folmes CD, Jaswal JS, Stanley WC (2010) Myocardial fatty acid metabolism in health and disease. Physiol Rev 90:207-258.

Makinoshima H, Takita M, Matsumoto S, Yagishita A, Owada S, Esumi H, Tsuchihara K (2014) Epidermal growth factor receptor (EGFR) signaling regulates global metabolic pathways in EGFR-mutated lung adenocarcinoma. J Biol Chem 289:20813-20823.

Min SH, Oh TJ, Baek SI, Lee DH, Kim KM, Moon JH, Choi SH, Park KS, Jang HC, Lim S (2018) Degree of ketonaemia and its association with insulin resistance after dapagliflozin treatment in type 2 diabetes. Diabetes Metab 44:73-76.

Mizuno M, Kuno A, Yano T, Miki T, Oshima H, Sato T, Nakata K, Kimura Y, Tanno M, Miura T (2018) Empagliflozin normalizes the size and number of mitochondria and

prevents reduction in mitochondrial size after myocardial infarction in diabetic hearts. Physiol Rep 6:e13741.

Mizuno Y, Harada E, Nakagawa H, Morikawa Y, Shono M, Kugimiya F, Yoshimura M, Yasue H (2017) The diabetic heart utilizes ketone bodies as an energy source. Metabolism 77:65-72.

Mudaliar S, Alloju S, Henry RR (2016) Can a shift in fuel energetics explain the beneficial cardiorenal outcomes in the EMPA-REG OUTCOME Study? a unifying hypothesis. Diabetes Care 39:1115-1122.

Münzel T, Gori T, Keaney JF Jr, Maack C, Daiber A (2015) Pathophysiological role of oxidative stress in systolic and diastolic heart failure and its therapeutic implications. Eur Heart J 36:2555-2564.

Murase H, Kuno A, Miki T, Tanno M, Yano T, Kouzu H, Ishikawa S, Tobisawa T, Ogasawara M, Nishizawa K, Miura T (2015) Inhibition of DPP-4 reduces acute mortality after myocardial infarction with restoration of autophagic response in type 2 diabetic rats. Cardiovasc Diabetol 14:103.

Nagao M, Toh R, Irino Y, Mori T, Nakajima H, Hara T, Honjo T, Satomi-Kobayashi S, Shinke T, Tanaka H, Ishida T, Hirata K (2016) β-Hydroxybutyrate elevation as a

compensatory response against oxidative stress in cardiomyocytes. Biochem Biophys Res Commun 475:322-328.

Neal B, Perkovic V, Mahaffey KW, de Zeeuw D, Fulcher G, Erondu N, Shaw W, Law G, Desai M, Matthews DR; CANVAS Program Collaborative Group (2017) Canagliflozin and cardiovascular and renal events in type 2 diabetes. N Engl J Med 377:644–657.

Nichols GA, Gullion CM, Koro CE, Ephross SA, Brown JB (2004) The incidence of congestive heart failure in type 2 diabetes: an update. Diabetes Care 27:1879-1884.

Niemann B, Rohrbach S, Miller MR, Newby DE, Fuster V, Kovacic JC (2017) Oxidative stress and cardiovascular risk: obesity, diabetes, smoking, and pollution: part 3 of a 3-part series. J Am Coll Cardiol 70:230-251.

Obokata M, Negishi K, Sunaga H, Ishida H, Ito K, Ogawa T, Iso T, Ando Y, Kurabayashi M (2017) Association between circulating ketone bodies and worse outcomes in hemodialysis patients. J Am Heart Assoc 6:e006885.

Satterstrom FK, Swindell WR, Laurent G, Vyas S, Bulyk ML, Haigis MC (2015) Nuclear respiratory factor 2 induces SIRT3 expression. Aging Cell 14:818-825.

Schugar RC, Moll AR, André d'Avignon D, Weinheimer CJ, Kovacs A, Crawford PA (2014) Cardiomyocyte-specific deficiency of ketone body metabolism promotes accelerated pathological remodeling. Mol Metab 3:754-769.

Shah AD, Langenberg C, Rapsomaniki E, Denaxas S, Pujades-Rodriguez M, Gale CP, Deanfield J, Smeeth L, Timmis A, Hemingway H (2015) Type 2 diabetes and incidence of cardiovascular diseases: a cohort study in 1·9 million people. Lancet Diabetes Endocrinol 3:105-113.

Shimazu T, Hirschey MD, Newman J, He W, Shirakawa K, Le Moan N, Grueter CA, Lim H, Saunders LR, Stevens RD, Newgard CB, Farese RV Jr, de Cabo R, Ulrich S, Akassoglou K, Verdin E (2013) Suppression of oxidative stress by β-hydroxybutyrate, an endogenous histone deacetylase inhibitor. Science 339:211-214.

Takada A, Miki T, Kuno A, Kouzu H, Sunaga D, Itoh T, Tanno M, Yano T, Sato T, Ishikawa S, Miura T (2012) Role of ER stress in ventricular contractile dysfunction in type 2 diabetes. PLoS One 7:e39893.

Tseng AH, Wu LH, Shieh SS, Wang DL (2014) SIRT3 interactions with FOXO3 acetylation, phosphorylation and ubiquitinylation mediate endothelial cell responses to hypoxia. Biochem J 464:157-168.

Uchihashi M, Hoshino A, Okawa Y, Ariyoshi M, Kaimoto S, Tateishi S, Ono K, Yamanaka R, Hato D, Fushimura Y, Honda S, Fukai K, Higuchi Y, Ogata T, Iwai-Kanai E, Matoba S (2017) Cardiac-specific bdh1 overexpression ameliorates oxidative stress and cardiac remodeling in pressure overload-induced heart failure. Circ Heart Fail 10:e004417

Udell JA, Cavender MA, Bhatt DL, Chatterjee S, Farkouh ME, Scirica BM (2015) Glucose-lowering drugs or strategies and cardiovascular outcomes in patients with or at risk for type 2 diabetes: a meta-analysis of randomised controlled trials. Lancet Diabetes Endocrinol 3:356-366.

Verma S, Rawat S, Ho KL, Wagg CS, Zhang L, Teoh H, Dyck JE, Uddin GM, Oudit GY, Mayoux E, Lehrke M, Marx N, Lopaschuk GD (2018) Empagliflozin increases cardiac energy production in diabetes. J Am Coll Cardiol Basic Trans Science 2018, in press.

Wentz AE, d'Avignon DA, Weber ML, Cotter DG, Doherty JM, Kerns R, Nagarajan R, Reddy N, Sambandam N, Crawford PA (2010) Adaptation of myocardial substrate metabolism to a ketogenic nutrient environment. J Biol Chem. 285:24447-24456.

Yin J, Han P, Tang Z, Liu Q, Shi J (2015) Sirtuin 3 mediates neuroprotection of ketones against ischemic stroke. J Cereb Blood Flow Metab 35:1783-1789.

Zinman B, Wanner C, Lachin JM, Fitchett D, Bluhmki E, Hantel S, Mattheus M, Devins T, Johansen OE, Woerle HJ, Broedl UC, Inzucchi SE; EMPA-REG OUTCOME Investigators (2015) Empagliflozin, Cardiovascular Outcomes, and Mortality in Type 2 Diabetes. N Engl J Med 373:2117-2128.

Footnotes

Financial support:

This study was supported by a grant from Boehringer Ingelheim, and a Research and Education Grant 2016-2017 from Sapporo Medical University. Boehringer Ingelheim did not play any role in the collection, analysis and interpretation of data or the writing of the manuscript.

Previous Presentation:

A part of this work was presented at the annual meeting of the European Association for the Study of Diabetes, Lisbon, Portugal, 11–15 September 2017.

Reprint request:

Tetsuji Miura, MD, PhD

Department of Cardiovascular, Renal, and Metabolic Medicine, Sapporo Medical University School of Medicine, South-1, West-16, Chuo-ku, Sapporo 060-8543, Japan.

Email: miura@sapmed.ac.jp

Figure Legends

Figure 1. Experimental protocols.

Experimental protocols for survival study and cardiac tissue sampling in empagliflozin experiments (A) and β-hydroxybutyrate experiments (B).

Figure 2. Effects of empagliflozin on survival rate, myocardial ATP and BNP after MI

(A) Kaplan-Meier survival analysis of LETO treated with a vehicle (LETO), LETO treated with empagliflozin (LETO+EMPA), OLETF treated with a vehicle (OLETF), and OLETF treated with empagliflozin (OLETF+EMPA). *p<0.05. (B) Kaplan-Meier survival analysis of OLETF treated with a vehicle (OLETF) and OLETF treated with β-hydroxybutyrate (OLETF+βOHB). (C) Infarct size measured at 48 hr after MI. (D) ATP level in the non-infarcted myocardium sampled 12 hr after MI. N= 6-7 in each group. *p<0.05. (E) BNP mRNA levels normalized to β-actin in the non-infarcted myocardium after MI. N= 8 in each group. *p<0.05. BNP= brain natriuretic peptide. a.u.= arbitrary unit.

Figure 3. Expressions of molecules regulating energy substrate metabolism

mRNA levels of GLUT1 (A), GLUT4 (B), PPARα (C), CD36 (D), CPT1b (E) and FoxO3a (F) in the myocardium. *p<0.05. N= 4-9 in each group. Representative immunoblot (left) and summary data (right) of BDH1 (G), SCOT (H), MCT1 (I) and CPT1b (J) protein levels normalized by vinculin in the non-infarcted myocardium after MI in LETO, OLETF and empagliflozin-treated OLETF

(OLETF+EMPA). N= 6-8 in each group. GLUT1= glucose transporter type 1, PPARα= peroxisome proliferator-activated receptor α, CD36= cluster of differentiation 36, CPT1b= carnitine palmitoyltransferase 1b, FoxO3a= forkhead box O3a, BDH1= 3-hydroxybutyrate dehydrogenase 1, SCOT= succinyl-CoA-3-oxaloacid CoA transferase, MCT1= monocarboxylate transporter. a.u.= arbitrary unit.

Figure 4. Summary of changes in metabolomics profile.

Metabolites of the energy production pathway (glycolysis, ketone and lipid oxidation, and TCA cycle) and pentose phosphate pathway. Concentrations of all metabolites are expressed as nmol/g wet tissue. *p<0.05. N=4 in each group. G6P= glucose 6-phosphate, F6P= fructose 6-phosphate, F1,6P= fructose 1,6-diphosphate, 3PG= 3-phosphoglyceric acid, GSH= reduced glutathione, GSSG=oxidized glutathione, R5P= ribose-5-phosphate, Ru5P= ribulose-5-phosphate, AcCoA= acetyl CoA, AAcCoA= acetoacetyl CoA, βOHB=β-hydroxybutyrate.

Figure 5. Effects of empagliflozin on lipid peroxidation and anti-oxidant proteins

(A) MDA+4HNE in the non-infarcted myocardium after myocardial infarction (MI) in LETO, OLETF and empagliflozin-treated OLETF (EMPA). N= 6-8 in each group. Representative immunoblot (left) and summary data (right) of SOD2 (B), catalase (C), acetylated histone H3 (D) and Sirt3 (E) protein levels normalized by vinculin in the non-infarcted myocardium after MI in LETO, OLETF and empagliflozin-

treated OLETF (OLETF+EMPA). *p<0.05. N= 6-8 in each group. MDA= malondialdehyde, 4HNE= 4-hydroxynonenal, SOD= superoxide dismutase, AcH3= acetylated histone H3, Sirt3= NAD^+-dependent deacetylase sirtuin-3. a.u.= arbitrary unit.

Figure 6. Effects of βOHB on lipid peroxidation and anti-oxidant proteins

(A) MDA+4HNE in the non-infarcted myocardium after MI in OLETF and β-hydroxybutyrate-treated OLETF (βOHB). *p<0.05. N= 6-8 in each group. Representative immunoblot (left) and summary data (right) of SOD2 (B), catalase (C) and Sirt3 (D) protein levels normalized by vinculin in the non-infarcted myocardium after MI in OLETF and β-hydroxybutyrate-treated OLETF (βOHB). *p<0.05. N= 6-8 in each group. MDA= malondialdehyde, 4HNE= 4-hydroxynonenal, SOD= superoxide dismutase, Sirt3= NAD^+-dependent deacetylase sirtuin-3.

Figure 7. A scheme of possible mechanisms by which SGLT2 inhibitors protect the myocardium from lethal heart failure after myocardial infarction

The mechanisms suggested by results of the present study is highlighted in blue. Glc Ox= glucose oxidation, FA Ox= fatty acid oxidation, Fis 1= fission 1, TGF= tubuloglomerular feedback.

Table 1.

Metabolic, hemodynamic and echocardiographic parameters before induction of MI

	LETO	LETO+EMPA	OLETF	OLETF+EMPA
Body weight (g)	524.7 ± 6.4	524.0 ± 7.7	645.0 ± 7.8 *	644.4 ± 6.2 †
Blood glucose (mg/dL)	124.2 ± 2.7	112.9 ± 3.6	170.7 ± 6.9 *	116.4 ± 6.4 ‡
βOHB (mmol/L)	0.77 ± 0.03	1.37 ± 0.07 *	0.62 ± 0.02 *	1.17 ± 0.08 †‡
Heart rate (bpm)	342.7 ± 6.4	330.2 ± 4.9	324.4 ± 5.6	326.8 ± 5.3
Mean BP (mmHg)	105.8 ± 2.6	100.6 ± 2.9	122.7 ± 3.3 *	120.3 ±2.1 †
FS (%)	44.2 ± 1.1	47.4 ± 1.1	45.4 ± 1.0	44.5 ± 1.0
IVST (mm)	1.72 ± 0.04	1.71 ± 0.04	1.73 ± 0.03	1.77 ± 0.03
PWT (mm)	1.82 ± 0.07	1.80 ± 0.05	1.83 ± 0.04	1.82 ± 0.08
LVEDD (mm)	8.36 ± 0.11	8.58 ± 0.18	8.86 ± 0.09 *	8.85 ± 0.09

Values are mean ± SEM. N= 17~27

* $p<0.05$ vs. LETO, † $p<0.05$ vs. LETO+EMPA, ‡ $p<0.05$ vs. OLETF

βOHB, β-hydroxybutyrate; BP, blood pressure; EMPA, empagliflozin;

FS, fractional shortening; IVST, interventricular septal thickness;

PWT, posterior wall thickness; LVEDD, left ventricular end-diastolic dimension

JPET Fast Forward. Published on December 14, 2018 as DOI: 10.1124/jpet.118.253666
This article has not been copyedited and formatted. The final version may differ from this version.

Table 2. Metabolic parameters at 12h after MI (before sampling)

	LETO	OLETF	OLETF+EMPA
Blood glucose (mg/dL)	135.9 ± 7.3	197.4 ± 9.1 *	114.9 ± 7.1 †
Serum insulin (ng/mL)	0.94 ± 0.04	1.27 ± 0.09 *	1.23 ± 0.08 *
βOHB (mmol/L)	1.08 ± 0.08	1.33 ± 0.14	4.20 ± 0.50 *†
Total cholesterol (mg/dL)	97.4 ± 5.1	116.3 ± 9.2 *	87.1 ± 4.6 †
Triglyceride (mg/dL)	21.6 ± 5.7	180.3 ± 25.6 *	118.2 ± 18.3 *†
pH	7.40 ± 0.02	7.44 ± 0.01	7.38 ± 0.02

Values are mean ± SEM. N= 11~16

* p<0.05 vs. LETO, † p< p0.05 vs. OLETF

βOHB, β-hydroxybutyrate; EMPA, empagliflozin; pH was measured by blood gas analysis

JPET Fast Forward. Published on December 14, 2018 as DOI: 10.1124/jpet.118.253666
This article has not been copyedited and formatted. The final version may differ from this version.

Table 3. Metabolic and hemodynamic parameters before MI in ketone infusion study.

	OLETF	
	Vehicle	βOHB
Body weight (g)	666.8 ± 6.1	663.1 ± 9.9
Blood glucose (mg/dL)	163.4 ± 7.4	143.5 ± 9.4
βOHB (mmol/L)	0.62 ± 0.03	0.82 ± 0.04 *
Heart rate (bpm)	318.4 ± 6.7	331.3 ± 8.8
Mean blood pressure (mmHg)	117.8 ± 2.3	109.2 ± 2.4 *

Values are mean ± SEM. N= 13-15

* $p<0.05$ vs. Vehicle

βOHB, β-hydroxybutyrate

JPET Fast Forward. Published on December 14, 2018 as DOI: 10.1124/jpet.118.253666
This article has not been copyedited and formatted. The final version may differ from this version.

Figure 1

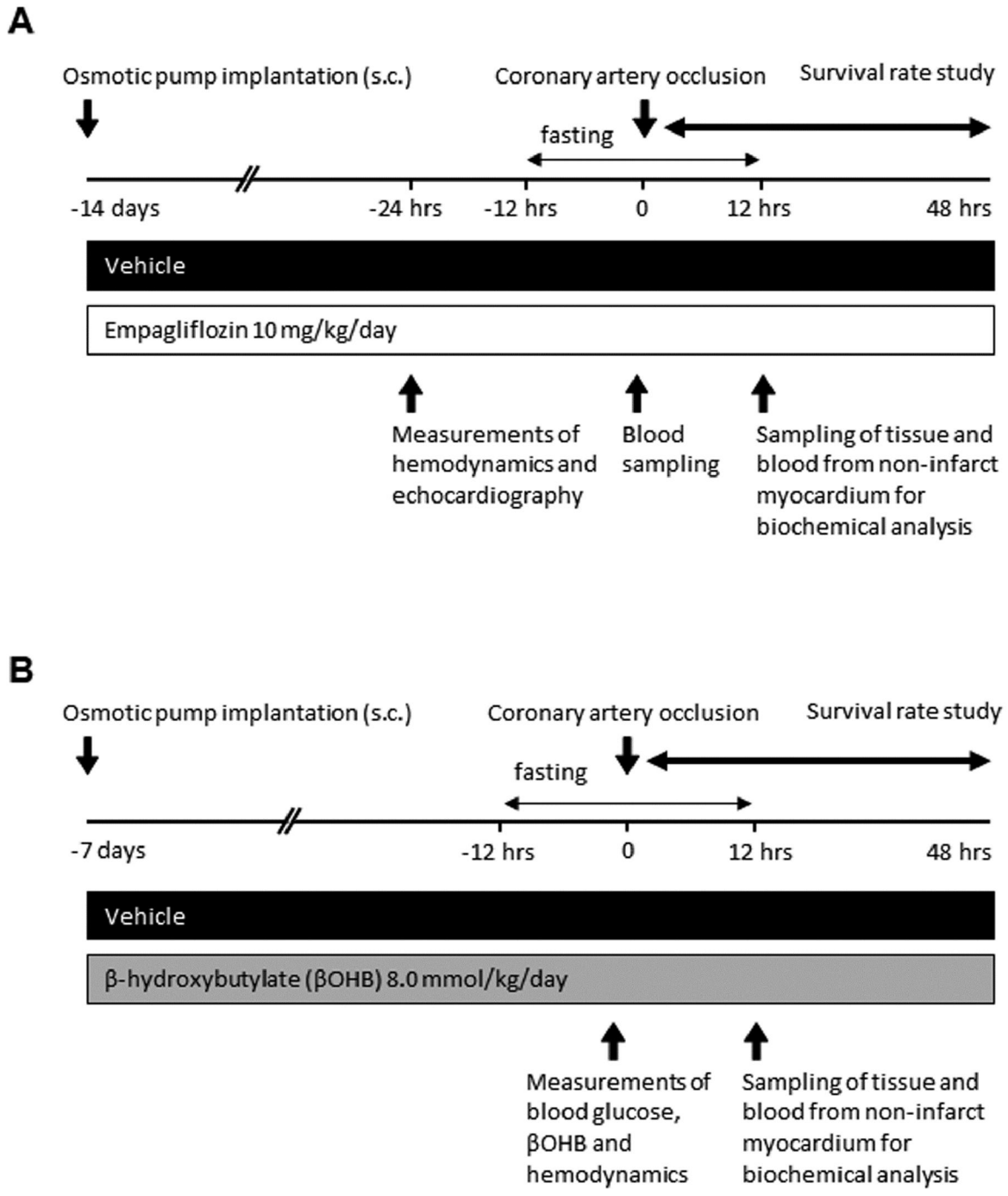

JPET Fast Forward. Published on December 14, 2018 as DOI: 10.1124/jpet.118.253666
This article has not been copyedited and formatted. The final version may differ from this version.

Figure 2

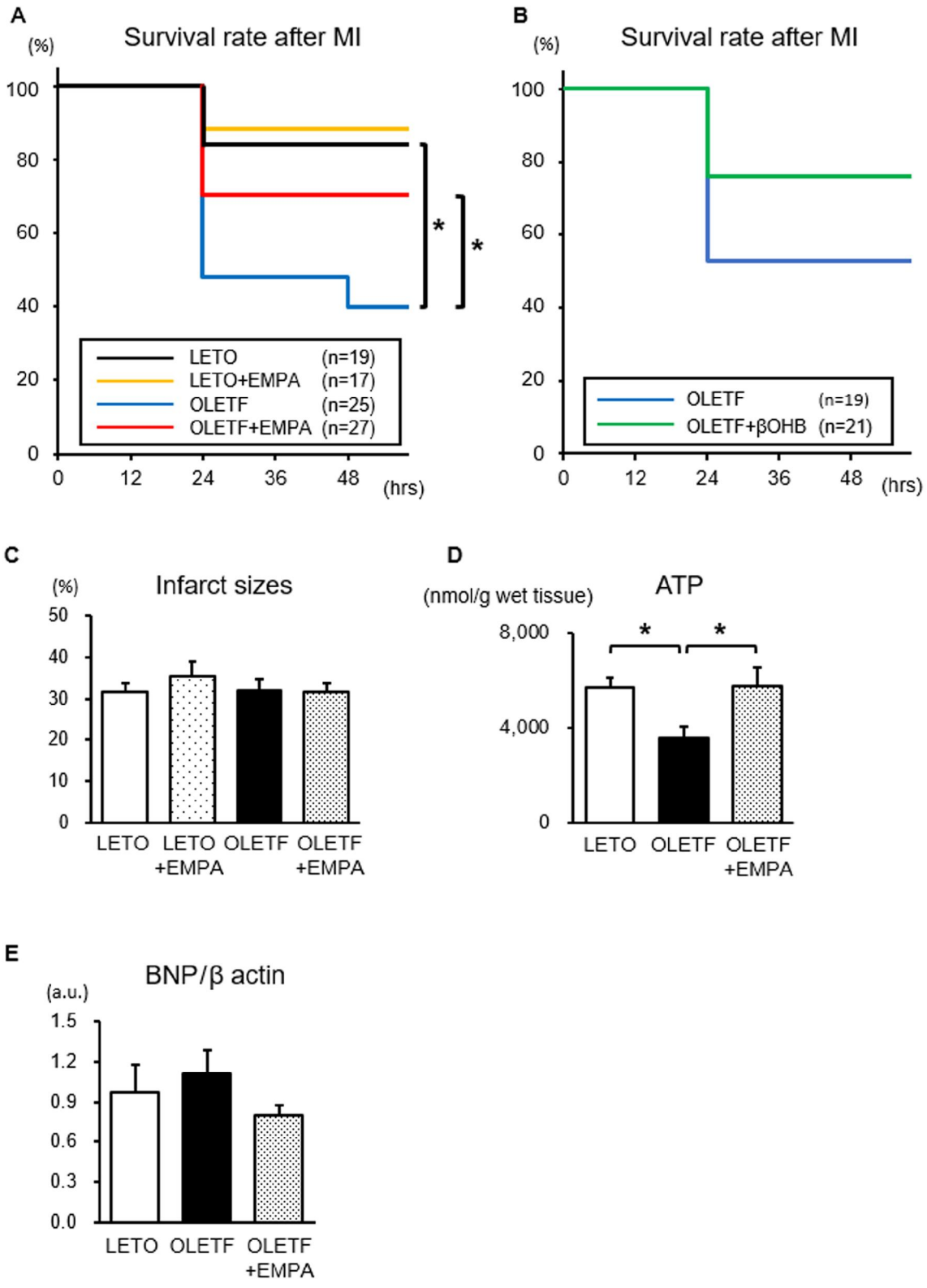

Figure 3

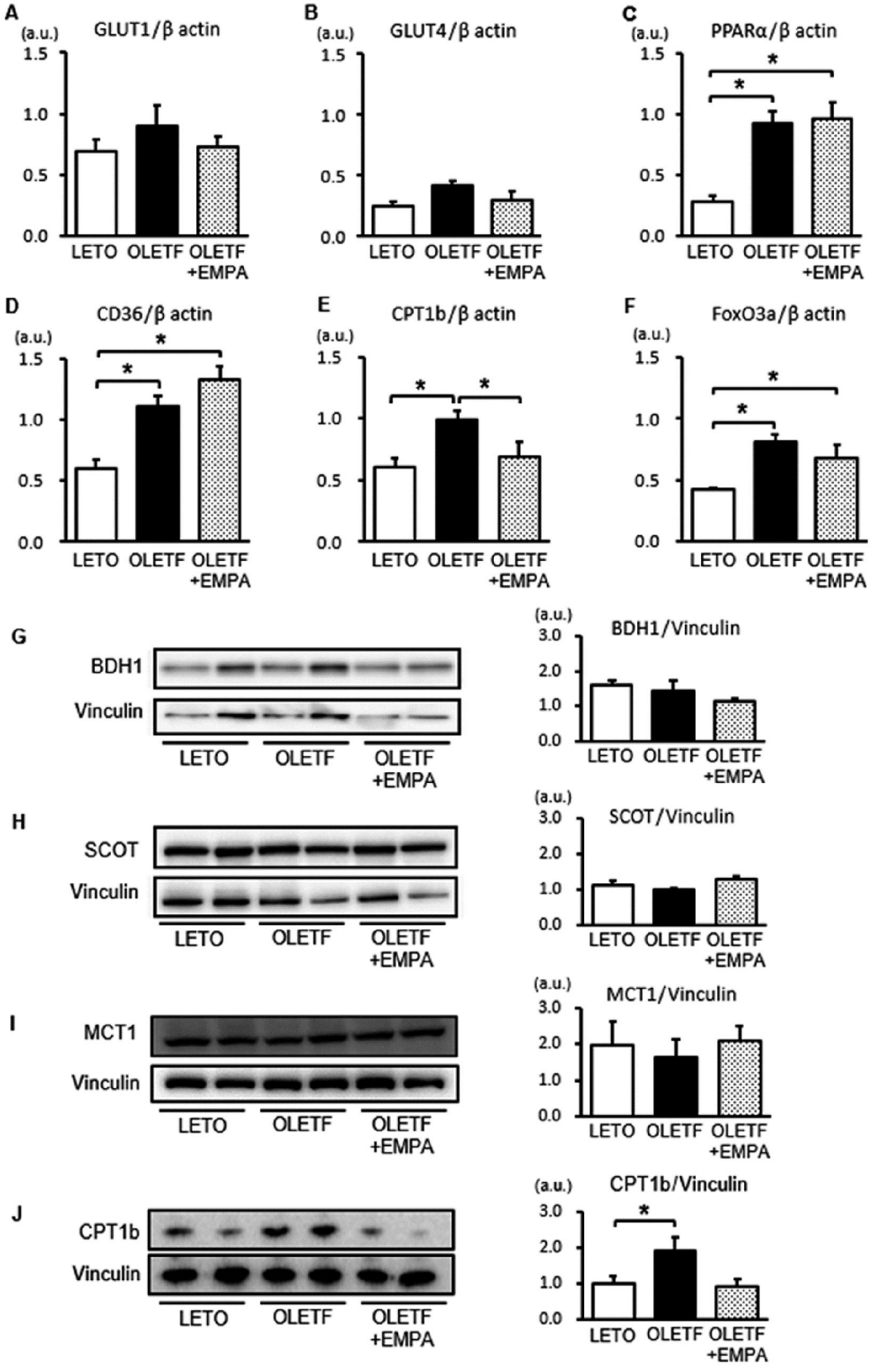

JPET Fast Forward. Published on December 14, 2018 as DOI: 10.1124/jpet.118.253666
This article has not been copyedited and formatted. The final version may differ from this version.

Figure 4

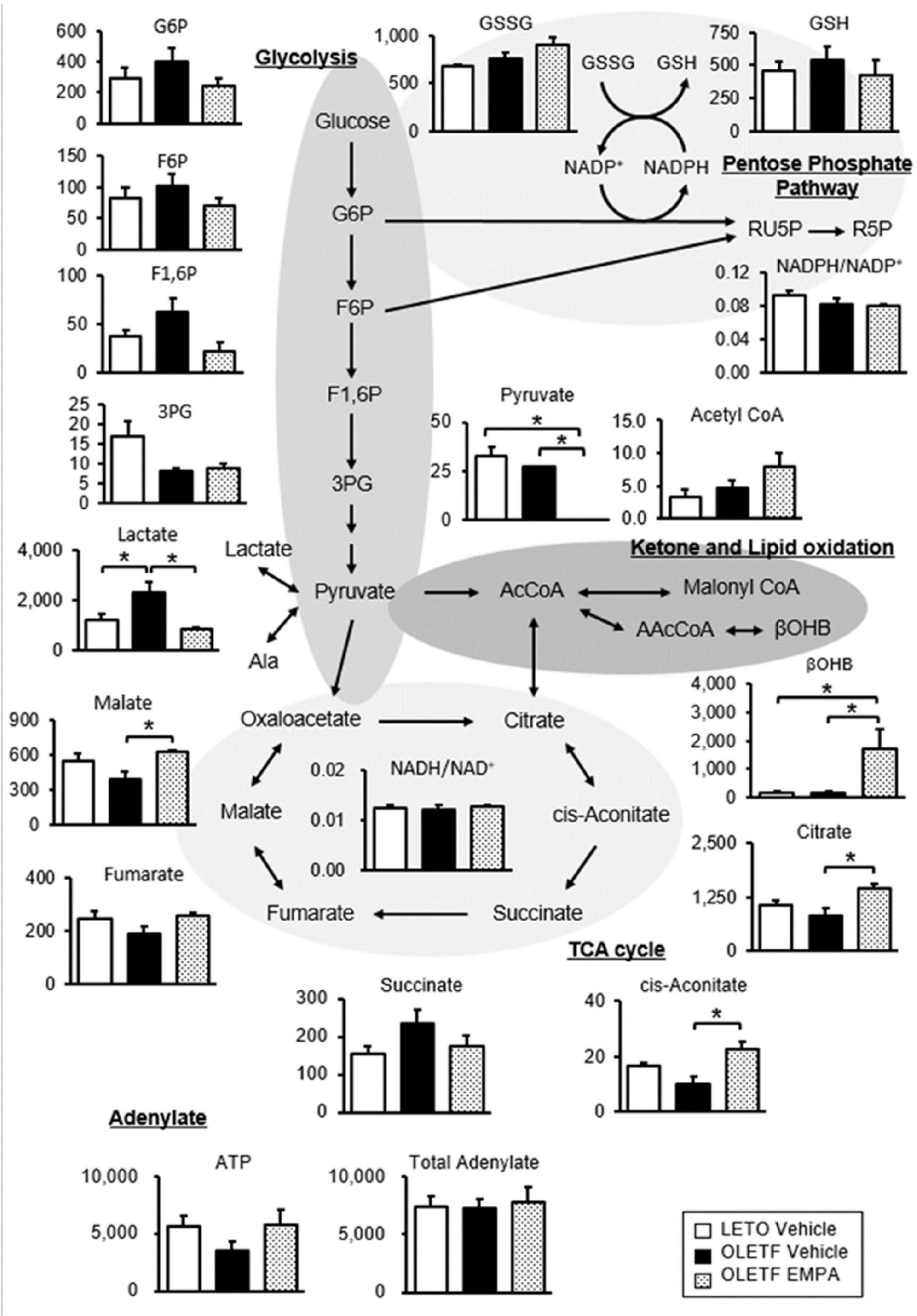

JPET Fast Forward. Published on December 14, 2018 as DOI: 10.1124/jpet.118.253666
This article has not been copyedited and formatted. The final version may differ from this version.

Figure 5

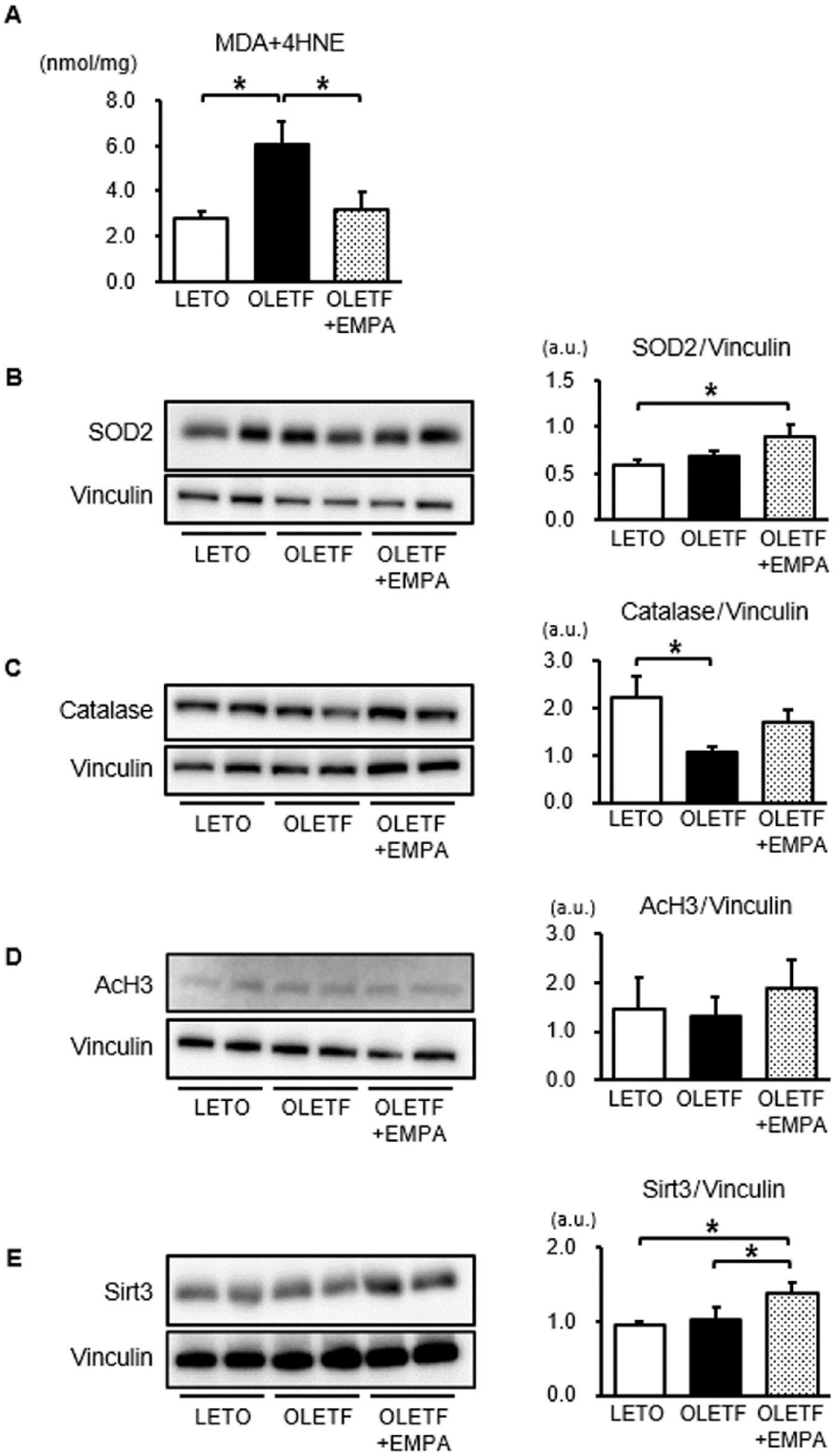

JPET Fast Forward. Published on December 14, 2018 as DOI: 10.1124/jpet.118.253666
This article has not been copyedited and formatted. The final version may differ from this version.

Figure 6

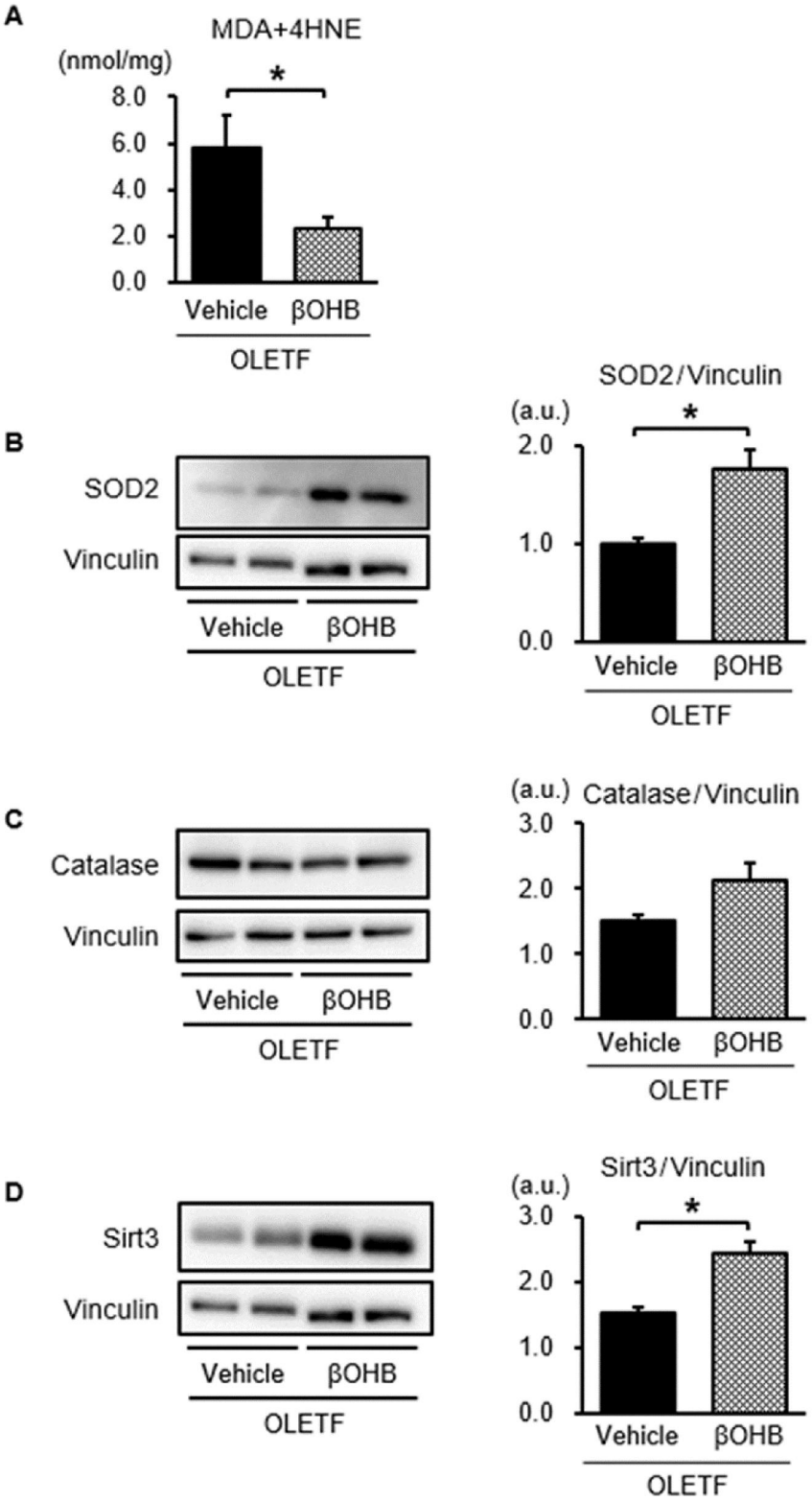

JPET Fast Forward. Published on December 14, 2018 as DOI: 10.1124/jpet.118.253666
This article has not been copyedited and formatted. The final version may differ from this version.

Figure 7

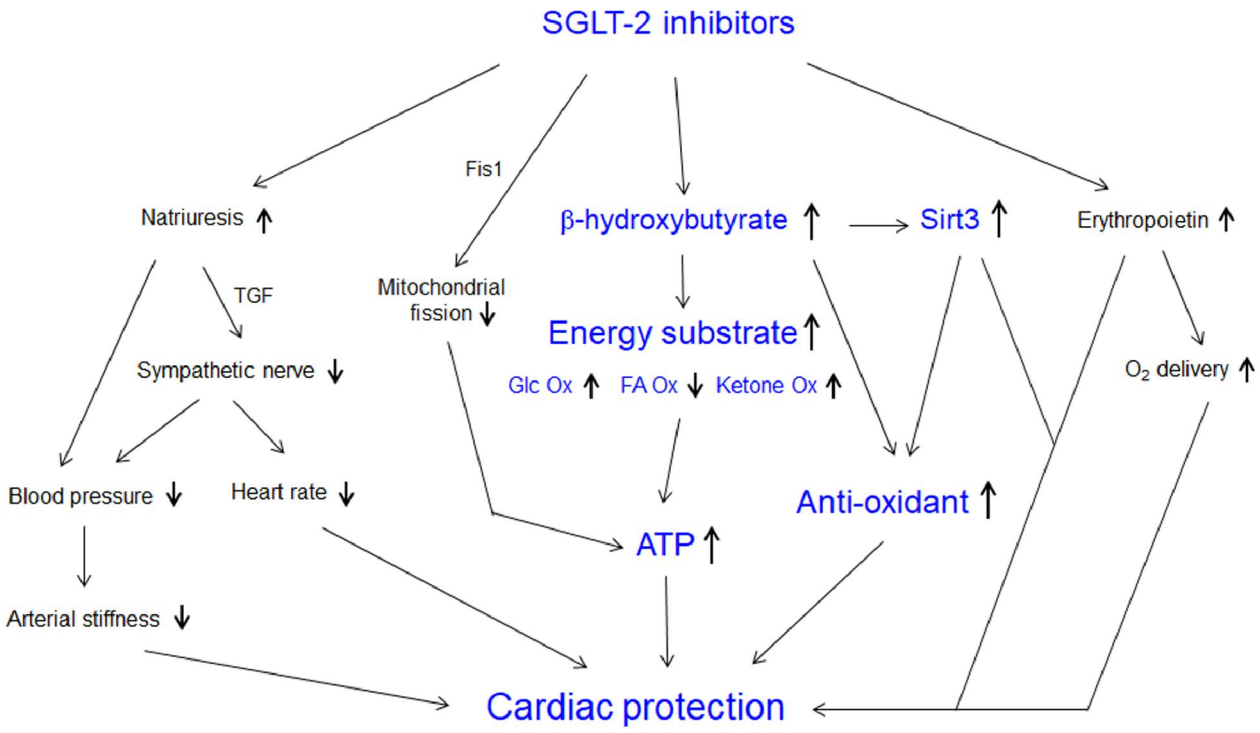

JPET/2018/253666

Supplemental Tables

Empagliflozin, an SGLT2 inhibitor, reduced the mortality rate after acute myocardial infarction with modification of cardiac metabolomes and anti-oxidants in diabetic rats.

Hiroto Oshima, Takayuki Miki, Atsushi Kuno, Masashi Mizuno, Tatsuya Sato, Masaya Tanno, Toshiyuki Yano, Kei Nakata, Yukishige Kimura, Koki Abe, Wataru Ohwada, Tetsuji Miura

Department of Cardiovascular, Renal and Metabolic Medicine (H.O., Ta.M., A.K., M.M., T.S., M.T., T.Y., K.N., Y.K., K.A., W.O., Te.M.), Department of Pharmacology (A.K.), and Department of Cellular Physiology and Signal Transduction (T.S.),
Sapporo Medical University School of Medicine, Sapporo, Japan.

Supplemental Table 1. Antibodies,Taqman gene expression assays and primer sequence

Antibodies	Source	Cat. No.
Rabbit polyclonal anti-BDH1	Proteintech	15417-1-AP
Rabbit polyclonal anti-SCOT	Proteintech	12175-1-AP
Rabbit polyclonal anti-MCT1	Abcam	ab93048
Rabbit polyclonal anti-SOD2	Merck Millipore	06-984
Mouse monoclonal anti-catalase	Sigma-Aldrich	C0979
Rabbit monoclonal anti-acetyl-Histone H3 (Lys9)	Cell Signaling Technology	#9649
Rabbit monoclonal anti-Sirt3	Cell Signaling Technology	#5490

Taqman gene expression assays	
BNP	Rn00676450_g1
GLUT1	Rn01417099_m1
GLUT4	Rn00562597_m1
PPARα	Rn00566193_m1
SGLT1	Rn01640634_m1
SGLT2	Rn00574917_m1
CPT1b	Rn00682395_m1
FoxO3a	Rn01441087_m1
β–actin	Rn00667869_m1

Primer sequences for a SYBR Green method	
CD36	forward: 5’-GGCTGTGTTTGGAGGCATTCT-3’
	reverse: 5’-CCCGTTTTCACCCAGTTTTTG-3’

Supplemental Table 2. Concentration of myocardial metabolites determined by metabolome analysis.

	LETO	OLETF	OLETF+EMPA
Amino acid			
Alanine	1412.8±107.1	1783.5±136.7	796.7±197.7 *†
Arginine	141.2±4.5	201.8±10.2 *	235.3±57.3
Asparagine	111.0±29.3	138.6±8.4	93.1±28.7
Aspartic acid	1268.4±93.6	795.9±118.9 *	892.0±311.6
Carnosine	69.7±4.7	29.9±2.1 *	31.1±4.6 *
Glutamic acid	6643.3±539.0	8442.0±688.1	9970.5±621.6 *
Glutamine	8602.2±514.7	9652.5±712.5	13007.6±980.8 *†
Glycine	436.4±17.1	290.0±15.7 *	312.9±93.3
Histidine	116.2±8.7	104.4±14.7	106.8±18.9
Hydroxyproline	38.4±1.3	29.0±1.7 *	25.6±1.8 *
Isoleucine	63.5±1.9	79.7±5.2 *	165.7±40.9
Leucine	152.5±2.5	175.8±6.0 *	327.6±70.9
Lysine	357.7±35.7	485.8±24.9 *	491.5±65.8
Methionine	33.2±1.1	38.8±0.6 *	32.3±1.4 †
Phenylalanine	71.6±3.2	88.6±4.5 *	99.8±17.9
S-Adenosylmethionine	41.0±3.1	36.7±1.4	34.5±3.0
Serine	377.3±55.4	179.9±21.3 *	236.1±146.8
Threonine	176.7±15.0	188.5±4.4	214.0±47.8
Tryptophan	38.0±2.2	37.6±0.7	50.4±4.3
Tyrosine	52.7±3.7	72.0±3.1	78.2±15.5
Valine	77.3±5.8	116.1±9.8 *	297.9±75.5
Choline			
Betaine	181.6±7.9	162.0±13.2	240.3±35.6
Choline	74.5±3.3	109.4±8.5 *	110.4±16.3
N,N-Dimethylglycine	6.3±0.9	5.4±0.8	6.6±0.7
Coenzyme			
Coenzyme A	20.9±2.4	24.3±3.4	14.3±4.9
NAD	748.9±20.3	786.3±43.3	761.6±22.3
NADH	9.3±0.3	9.5±0.3	9.6±0.7
NADP	73.5±3.9	82.2±5.4	82.0±5.4

NADPH	6.7±0.3	6.6±0.4	6.5±0.9
β-Alanine	26.3±2.4	20.3±2.1	18.9±1.1 *
Energy			
ADP	1197.5±374.5	1957.7±200.0	1171.8±477.4
AMP	580.4±280.9	1804.1±571.9	879.7±678.1
ATP	5692.4±804.3	3571.4±725.5	5790.5±1237.9
GDP	25.7±7.3	52.7±6.6 *	28.0±9.8
GMP	14.7±6.6	43.7±10.1	18.0±11.0
GTP	139.1±17.3	117.7±18.2	150.6±31.3
Fatty acid			
Carnitine	852.6±66.3	1150.9±28.6 *	552.4±230.0
Glutathione			
Reduced glutathione (GSH)	460.4±72.4	542.2±105.3	419.5±120.9
Oxidized glutathione (GSSG)	670.2±22.9	758.8±66.0	890.1±92.2
Glycogen			
UDP-glucose	47.1±2.4	61.4±2.0 *	42.8±6.9
Galactose 1-phosphate	5.8±0.7	5.3±0.8	2.6±0.8 *
Glycolysis			
2-Phosphoglyceric acid	1.9±0.4	1.2±0.0	1.2±0.1
2,3-Diphosphoglyceric acid	43.4±3.8	35.9±5.6	37.3±3.3
3-Phosphoglyceric acid	16.8±4.0	8.3±0.5	9.0±1.1
Acetyl CoA	3.3±1.2	4.7±1.3	7.9±2.1
Dihydroxyacetone phosphate	16.4±4.3	8.1±2.6	3.5±2.1
Fructose 1,6-diphosphate	37.5±6.7	62.3±13.6	21.2±9.5
Fructose 6-phosphate	82.1±16.5	101.1±20.3	70.5±11.0
Glucose 1-phosphate	23.1±5.0	31.5±7.3	20.6±4.9
Glucose 6-phosphate	293.5±68.1	402.6±92.1	243.6±45.3
Glycerol 3-phosphate	114.8±35.5	177.5±44.6	57.4±12.9
Lactic acid	1250.1±205.4	2320.5±454.4 *	853.7±108.6 †
Phosphoenolpyruvic acid	3.5±1.5	0.5±0.2	1.5±0.4
Pyruvic acid	32.4±5.2	27.2±0.3	N.D.
Ketone			
α-Hydroxybutyric acid	11.9±1.4	13.0±2.5	31.0±5.9 *†
β-Hydroxybutyric acid	189.5±32.9	184.2±31.1	1719.0±669.5 *†

Pentose phosphate pathway			
6-Phosphogluconic acid	2.5±0.2	1.9±0.1	2.2±0.2
Ribose 1-phosphate	5.8±2.7	6.6±1.4	6.1±0.8
Ribose 5-phosphate	2.5±0.9	1.1±0.2	2.1±0.6
Ribulose 5-phosphate	5.7±1.4	4.5±0.3	5.1±1.0
Polyamine			
Putrescine	12.1±0.9	8.1±2.5	11.0±2.0
Spermidine	19.4±0.9	20.7±3.3	17.4±1.1
Spermine	14.1±0.5	18.4±2.2	11.5±0.9 †
Purine			
Adenine	4.0±0.5	3.2±0.3	2.9±0.2
Adenosine	75.3±19.7	98.4±9.5	53.6±15.8
Adenylosuccinic acid	3.2±0.8	3.2±0.7	2.9±0.3
ADP-ribose	15.8±3.4	9.4±0.9	13.3±3.5
Hypoxanthine	6.7±2.1	4.8±0.9	3.5±0.1
Inosine	88.1±24.9	128.2±20.4	66.9±9.9 †
Inosine 5-monophosphate (IMP)	56.6±11.4	52.6±9.2	36.3±11.8
Uric acid	7.0±0.5	10.6±2.8	8.0±2.8
Xanthine	1.4±0.5	1.6±0.2	2.6±1.3
Signal			
cAMP	1.2±0.1	1.0±0.1	0.9±0.0
TCA cycle			
2-Hydroxyglutaric acid	9.7±1.2	8.4±0.9	10.4±1.2
cis-Aconitic acid	16.3±1.3	10.2±2.7	22.3±2.8 †
Citric acid	1063.9±97.7	826.2±180.2	1436.7±121.6 †
Fumaric acid	246.6±27.7	188.5±27.7	256.3±11.2
Malic acid	552.1±58.8	393.1±64.1	624.0±20.2 †
Succinic acid	155.1±20.1	236.3±35.8	176.4±24.4
Urea			
Argininosuccinic acid	14.7±0.3	13.7±0.7	16.1±1.0
Citrulline	34.6±3.0	40.4±3.7	49.0±8.0
Creatine	13408.5±742.9	13115.2±653.0	12308.3±339.2
Creatinine	34.2±1.8	26.9±1.0 *	23.3±1.9 *
Ornithine	22.1±0.9	20.0±0.9	39.2±16.1

Phosphocreatine	330.7±150.8	28.4±7.3	50.2±10.4
Urea	5042.5±243.9	5430.1±343.5	6762.8±192.4 *†

Values are mean±SEM (nmol/g wet tissue).

* $p<0.05$ vs. LETO. † $p<0.05$ vs. OLETF